Electronic Supplementary Material (ESI) for Chemical Communications.

Nickel oxide-decorated in-situ grown 3-D graphitic forest engrained carbon foam electrode for microbial fuel cell

Shiv Singh,*‡[a] Amol Pophali,‡[b] Rishabh Anand Omar,[b] Rajeev Kumar[a], Pradip Kumar,[c] Dehi Pada Mondal,[a] Deepak Pant*[d] and Nishith Verma*[b]

[a]Lightweight metallic materials, Council of Scientific and Industrial Research- Advanced Materials and Processes Research Institute, Bhopal - 462026, India
[b]Department of Chemical Engineering, Indian Institute of Technology Kanpur, Kanpur- 208016, India.
[c]Integrated Approach for Design and Product Development Division, CSIR-Advanced Materials and Processes Research Institute, Habibganj Naka, Hoshangabad Road, Bhopal, Madhya Pradesh, 462026, India.
[d]Separation and Conversion Technology, Flemish Institute for Technological Research (VITO), Boeretang 200, 2400 Mol, Belgium.
‡These authors contributed equally to this work

*Corresponding authors
Dr. Nishith Verma; email id: vermanishith@gmail.com; nishith@iitk.ac.in
Dr. Deepak Pant; email id: deepak.pant@vito.be
Dr. Shiv Singh: email id: sshiv.singh@ampri.res.in; sshiviitk@gmail.com

Synthesis of electrodes

The CF substrate is prepared by first dissolving the phenolic resin in acetone, and then, impregnating a polyurethane foam slab (size 20 x 20 x 10 mm^3) with resin solution. Next, the resin-impregnated foam is dried at 80 °C for the removal of excess acetone from the foam surface, and then stabilized at 250 °C in an air-atmosphere for increasing the cross-linking of the polymeric chains in resin. The stabilized foam is carbonized at 1000 °C in an argon gas atmosphere to prepare CF.

Active NiO nanoparticles after CNF-growth

Atomic absorption spectroscopy (AAS) was used to determine the total Ni loading in NiO-CNF-CF using acid digestion method [S1]. Based on the AAS measurements of the metal in the acid-digested/leached liquid samples, the NiO loading in NiO-CNF-CF was calculated to be 99.56 mg/g. Next, the material was sonicated in a 0.05 M HNO_3 solution for 5 min to dislodge the NiO nanoparticles from the tips of the CNFs [S2]. The metal-leached acid solution was then subjected to the AAS analysis to determine the Ni loading, and the NiO loading was calculated to be 55.27 mg/g. The atomic absorption spectroscopy (AAS) (Varian AA-240, USA) analysis also showed that that ~56% of the total NiO nanpoarticles in NiO-CNF-CF were exposed at the tips of the CNFs, whereas the remaining nanoparticles remained dispersed over the CF substrate. The surface-adhered NiO nanoparticles also facilitate electron transfer in CF. Here, it is also important to mention that the CVD temperature (~650 °C) used for the CNF-growth was significantly lower compared to the melting point (~1950 °C) of NiO. Therefore, all NiO NPs that were located at the tips of the CNFs may be considered to be active.

Elemental mapping

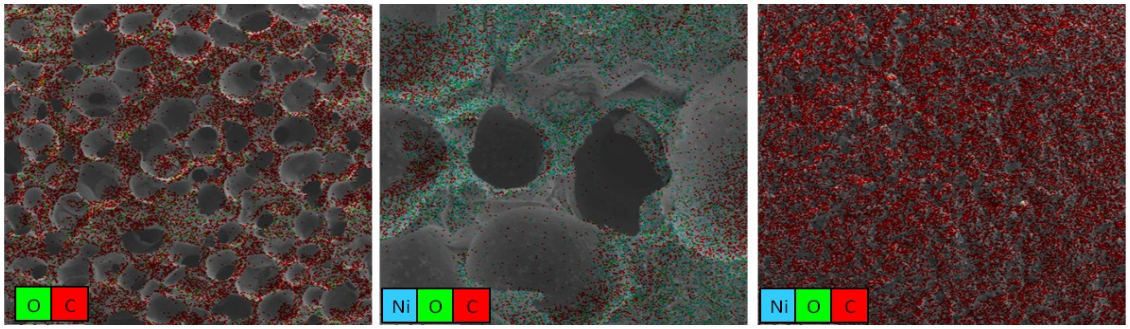

Fig. S1 Elemental mapping of (a) CF, (b) NiO-CF, and (c) NiO-CNF-CF

Fig. S1 shows the elemental mapping of the fabricated samples. The elements present in the electrodes were uniformly distributed over the electrode surface. Fig. S1a confirms the presence of carbon (C) and oxygen (O) in CF. Fig. S1b confirms the presence of nickel (Ni) in NiO-CF. Fig. S1c shows an abundant surface coverage of carbon (red) in NiO-CNF-CF, attributed to the growth of 3-D CNFs catalyzed by the NiO nanoparticles. Ni and O were also detected in NiO-CNF-CF.

HR-TEM analysis

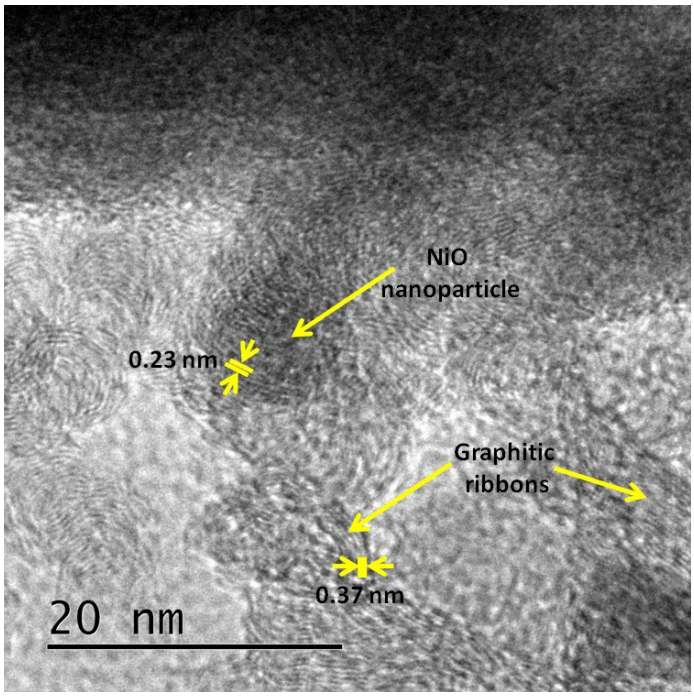

Fig. S2 HR-TEM image of NiO-CNF-CF

The high-resolution TEM image of NiO-CNF-CF is shown in Fig. S2 confirming the presence of NiO nanoparticles and CNFs in the material. The fully developed polycrystalline fringes were observed with a fringe spacing of ~0.23 nm corresponding to the (2 0 0) plane of NiO in the cubic phase [S3]. The graphitic ribbons of the 3-D CNFs were also evident. An approximate width of ~0.37 nm was observed for the carbon fringes, which was consistent with the d-spacing of (0 0 2) plane of graphitic carbon [S4]. The measured fringe-width, approximately equal to that of natural graphite (~0.33 nm), indicates that the NiO nanoparticles did not greatly affect the orientation of the graphitic carbon layers and the nanoparticles were synergistically bounded by the graphitic

CNFs. The HR-TEM data for the NiO and carbon fringes were consistent with the XRD analysis (Fig. 2a).

Thermal and Compressive strength

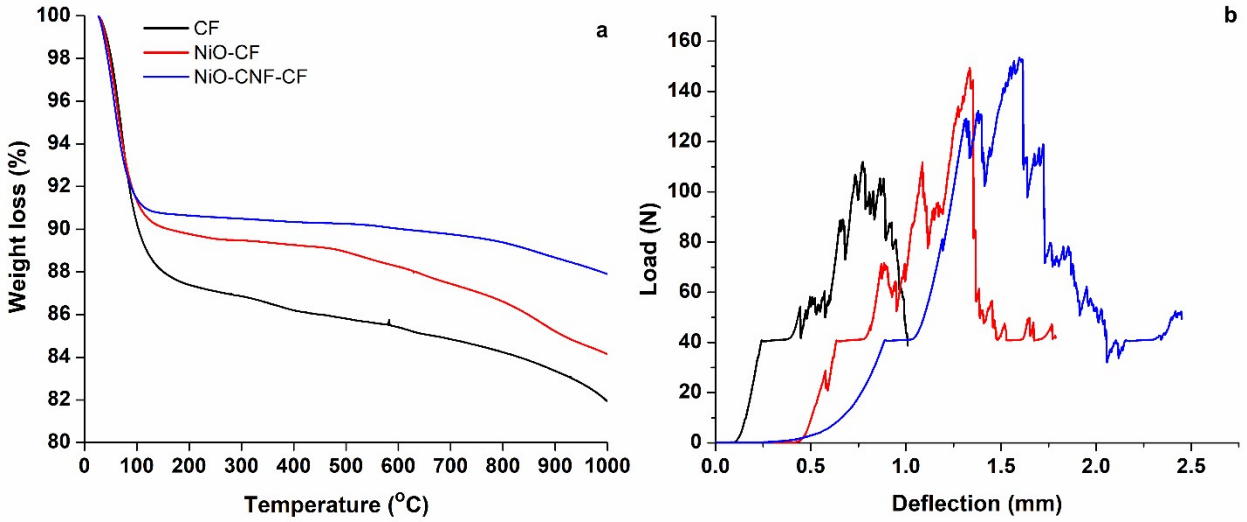

Fig. S3 (a) TGA and (b) load deflection graphs of CF, NiO-CF and NiO-CNF-CF electrodes

Fig S3(a) shows the TGA analysis of prepared electrodes. The data were expressed in percentage weight-loss of the materials with increasing temperatures. An initial 9% weight loss at temperatures up to 100 °C was observed in all materials and was attributed mainly to outgassing of moisture. Further, the respective weight-losses in CF, NiO-CF and NiO-CNF-CF were measured to be ~18.5, 16, and 12.3%, respectively over 100 – 1000 °C. Thus, calcination at 400 °C and CVD at 650 °C resulted in the relatively lower weight-loss in NiO-CNF-CF. Fig. S3(b) shows the load-deflection graph of the CF-based electrodes. The load-carrying capacity of the materials increased with the inclusion of NiO and CNF. NiO acted as a particle-reinforcement and increased the load-carrying capacity by 36% relative to that of the bare CF. The inclusion of the CNFs in NiO-CF also increased the load-carrying capacity, although marginally. The flexible CNFs act as a backbone to the rigid CF, thereby increasing the strength of CF. The load carrying capacity of NiO-CNF-CF is 40% greater than that of CF.

The BET surface area (S_{BET}) and total pore volume (V_T) of CF were determined to be 1.1 $m^2\ g^{-1}$ and 0.0012 $cm^3\ g^{-1}$, respectively (Table S1). The pore size distribution (PSD) data revealed that CF was majorly meso-macroporous. Post the impregnation and calcination steps, NiO nanoparticles were self-assembled to form a flaked rice-like structure (Fig. 1e), and therefore, the increased S_{BET} (143.3 $m^2\ g^{-1}$) and V_T (0.108 $cm^3\ g^{-1}$) were measured in NiO-CF. Growth of the CNFs increased the S_{BET} and V_T to 262.8 $m^2\ g^{-1}$ and 0.184 $cm^3\ g^{-1}$, respectively in NiO-CNF-CF. An interesting thing to note was that porosity developed in the materials (the transition referred in Fig. 1b,e,h) because of the NiO nanoparticles and CNFs. As shown later, the material porosity contributed to the high electrochemical activity.

Table S1

S_{BET}, VT and PSD of the prepared materials.

Material	S_{BET} ($m^2\ g^{-1}$)	V_T ($cm^3\ g^{-1}$)	PSD (%)		
			Micro	Meso	Macro
CF	1.1	0.0012	7.93	17.50	74.58
NiO-CF	143.3	0.108	88.49	6.66	4.85
NiO-CNF-CF	262.8	0.184	82.07	12.24	5.70

Cyclic voltammetry

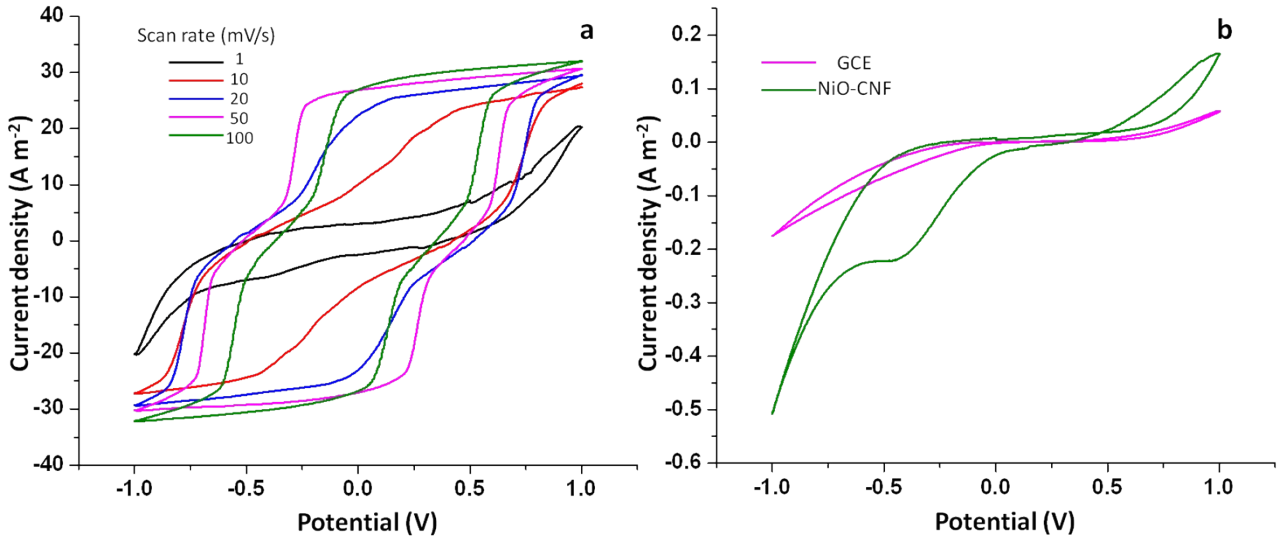

Fig. S4 Cyclic voltammograms of (a) NiO-CNF-CF at different scan rates, (b) NiO-CNF coated over GCE.

A quasi-rectangular electrochemical double-layer capacitive (EDLC) type CV plot (Fig. S4a) was recorded at 1 mV s^{-1}. As the scan rate was increased to 10 and 20 mV s^{-1}, the broad redox peaks were observed showing some contribution from the Faradaic currents. The characteristics of the CV curves further changed till the scan rate of 50 mV s^{-1}. The CV curves showed similar trend at 100 mV s^{-1}. The clearly visible redox peaks confirmed the pseudocapacitive bahaviour of the electrode. Thus, an optimized scan rate of 50 mV s^{-1} was used to carry out further analysis.

CV was also performed on NiO-CNF to determine its individual electrocatalytic activity in the absence of carbon foam. For this purpose, a small amount of NiO-CNF was dispersed in ethanol, and the mixture was coated on the glassy carbon electrode (GCE). The analysis parameters were the kept same as in the other CV measurements. Fig. S4b shows the CV curves for GCE (blank) and the NiO-CNF-coated GCE. The CV curve for blank GCE showed small capacitive currents. On the other hand, CV plots for NiO-CNF clearly showed a significant reduction peak with increasing currents (majorly because of Faradaic currents). Thus, it can be concluded that the capacitive characteristics of NiO-CNF-CF originated from the porosity in the material.

SEM images of biofilm

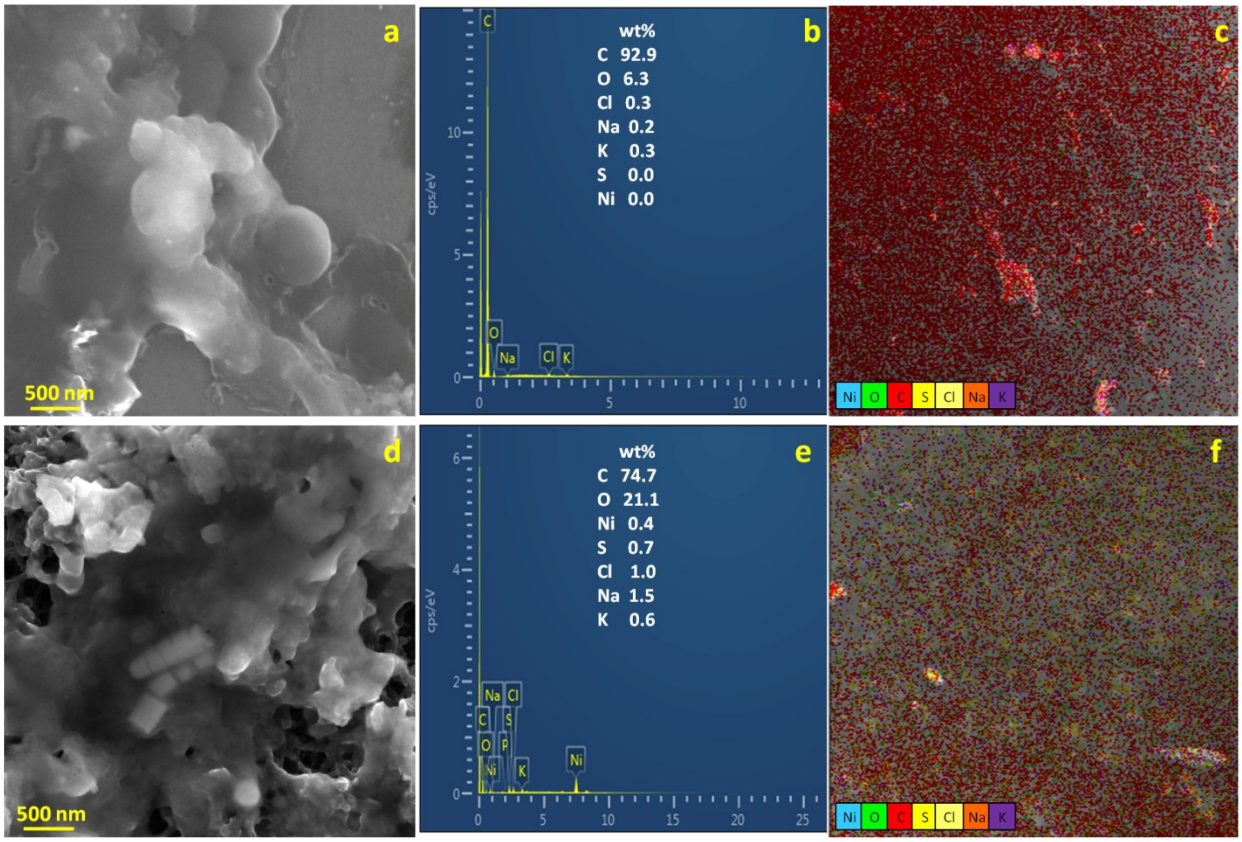

Fig. S5 SEM images of biofilm, EDX spectra and elemental mapping for spent electrode: (a-c) CF, and (d-f) NiO-CNF-CF

The electrodes were also analyzed post MFC operation using SEM-EDX analysis to ascertain its biocompatibility. It is evident from Fig. S5a that a thin layer of biofilm was formed uniformly over the CF electrode surface, whereas a dense, thick and uniformly distributed biofilm was found to be grown over the NiO-CNF-CF electrode (Fig. S5d). A dense and uniform biofilm is expected for high MFC performance. Therefore, NiO-CNF-CF can be termed as biocompatible and be efficiently used in MFC operations. The EDX spectra of spent electrodes (Fig. S5b, e) of both the MFC batches showed the presence of ions (S, Cl, Na and K) which were absorbed during the operation from the electrolytes. Fig. S5e shows significant amount of Ni confirming the presence of NiO nanoparticles within the electrode. Also, we carried out the AAS analysis of both anolyte and catholyte after the MFC operation. NiO were not detected in the electrolyte. Thus, leaching of

NiO nanparticles from the electrode to the electrolyte was not observed which supports the stability analysis discussed further. The uniform distribution of the elements without any agglomeration was observed in the elemental mapping of the electrodes after the MFC process (Fig. S5c, f)

Stability analysis

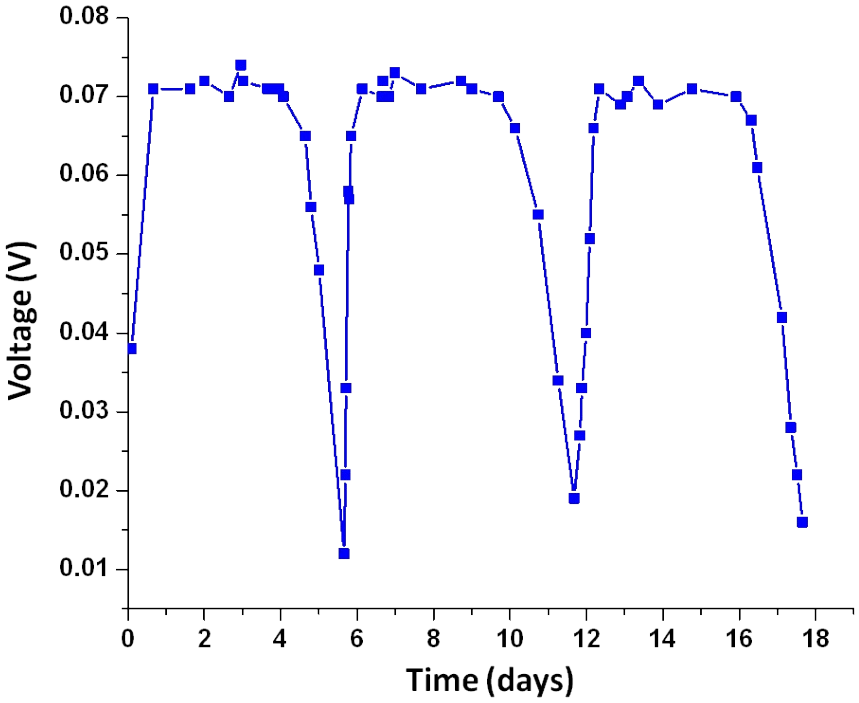

Fig. S6 Voltage-time plot for the NiO-CNF-CF-based MFC operated for ~18 days, indicating stability of the electrode.

Stability of the fabricated NiO-CNF-CF electrode was also determined in an MFC operation for ~18 days, using an external load of 100 Ω. Fig. S6 presents the voltage-time data. Three reproducible voltage-time cycles were recroded. The MFC achieved a voltage of ~0.071 V in ~0.6 days which remained almost constant till ~4 days. Further, the cell voltage gradually decreased to ~0.012 V because of consumption of the essential nutrients from the anolyte. The used electrolytes were then replaced with the fresh electrolytes for the next cycle. In the second cycle, the MFC re-attained the voltage of ~0.070 V in ~0.6 days and the voltage-time pattern approximately followed the previous cycle. The third cycle also followed the similar pattern. Thus, the electrode showcased its stability during the cell operation, indicating its suitability for multiple cycles. Also, the AAS

analysis of both anolyte and catholyte after the MFC operation was performed. No significant amount of NiO was detected or measured in the electrolyte. It is also evident from the EDX analysis (Fig. S5e) of NiO-CNF-CF post MFC-run that the amount of NiO remained approximately constant.

Coulombic efficiency calculations

The % COD reduction is calculated as follows:

$$\%\ COD\ reduction = \left(\frac{CODf - CODi}{CODi}\right) \times 100 \quad (1)$$

where, COD_i is the initial COD concentration and COD_f is the final COD concentration after each batch.

Total coulombs generated by the MFC over time:

$$Cp = \int_0^t Idt \quad (2)$$

Theoretical amount of coulombs that is available from COD:

$$ct = \frac{FbV(CODf - CODi)}{M} \quad (3)$$

where, F is the Faraday's constant (96,485 C mol^{-1} of electrons), *b* is the number of electrons per mole of substrate (*b* = 4), V (L) is the volume of electrolyte, M is the molecular weight of the substrate (M = 32 g mol^{-1}).

Coulombic efficiency (η_{CE}) is calculated as:

$$\eta CE = \left(\frac{Cp}{Ct}\right) \times 100 \quad (4)$$

References

[S1] B. Bhaduri and N. Verma, J Colloid Interface Sci., 2015, **457**, 62-71.
[S2] A.K. Gupta, D. Deva, A. Sharma and N. Verma, Ind. Eng. Chem. Res., 2010, **49**, 15, 7074-84.
[S3] G. Zhu, C. Xi, H. Xu, D. Zheng, Y. Liu, X. Xu and X. Shen, RSC Adv., 2012, 2, 4236-4241.
[S4] S.-J. Hwang, G.-O. Kim, S.-R. Yun and K.-S. Ryu, Electrochimica Acta, 2012, 78, 406-411.(1)